



Comparison and Revision of the Earthquake Early Warning Methods for Different Regional Seismic Data

Z. Wang⁽¹⁾, B. Zhao⁽²⁾

⁽¹⁾ PhD Student, Beijing Jiaotong University, zjwang8911@hotmail.com

⁽²⁾ Professor, Beijing Jiaotong University, bmzhao@bjtu.edu.cn

Abstract

Earthquake early warning (EEW) system is one of the most useful tools to mitigate seismic hazards. Although EEW methods have already been developed worldwide, the applicability of these processes in China is still unclear. Therefore, we tested and compared these methods by applying them to the seismic data recorded at the western area of China and attempted to provide a revised model for the earthquake early warning. The adopted data herein mainly consisted of the main-shock and aftershocks of the 2008 M_s 8.0 Wenchuan earthquake, where hundreds of three-component acceleration waveforms were treated to investigate the early warning theories. For the purpose of an EEW, reliable techniques for automatic seismic phases' identification are essential for the subsequent real-time analysis, thus we combined the short-term and long-term average ratio (STA/LTA CF) detector with the AIC function of higher order statistics to lock on the phase with a higher accuracy. Because the estimation of the event magnitude is the central objective of EEW, comparison and selection of the parameters including the average ground motion period τ_c and the cumulative absolute velocity (CAV) were investigated according to their performance as magnitude estimators. Then we established the regression relationship using our dataset and the impacts of the geological conditions and earthquake occurrence environments on the earthquake early warning were also studied.

Keywords: earthquake early warning; regional earthquake; P-wave detection; magnitude estimation

1. Introduction

Earthquake Early Warning (EEW) system provides alerts within a few seconds to tens of seconds for unfolding ground motions so that appropriate measures can be taken immediately to against seismic hazards [1, 2], e.g., critical facilities of industries can be shut off and the running trains can be slowed down before peak ground motion arrivals, preventing severe losses of life and property damage.

For the purpose of the EEW, reliable techniques for automatic detection of the initial portion of P wave are essential for subsequent real-time analysis as these phases can be used to determine the magnitude and location of an earthquake before destructive energy arrivals. Thus algorithm for automatic phase picking is the first step to extract events in real-time and high precise detection is necessary for urban and transport noise environment.

In EEW studies, period parameters such as the average ground motion period τ_c and dominant ground motion period τ_p^{\max} are among the most important parameters for rapid magnitude estimation [3, 4]. Many studies have shown that the period parameters are robust estimators of magnitude, as Olson and Allen [5] argued that the eventual magnitude of the event can be deterministic partially with the first few seconds after the P arrival but this interpretation remains controversial. Apart from that, the EEW system in Istanbul [6] regards the cumulative absolute velocity (CAV) as a rapid detector for strong ground motions and determines a damaging earthquake by some selectable thresholds. Since the CAV can reflect seismic duration and frequency content of an event, it is interesting to investigate if it can well correlated with magnitudes.

A robust input database is essential to generate reliable detecting method and regression functions for magnitude estimation by using a statistical approach. The 2008 M_s 8.0 Wenchuan earthquake occurred in Sichuan Province provided us sound data for such studies. In this paper, we first used a two-step algorithm to pick early portions of P waveforms recorded near large faults and earthquake rupture zones by combining the short-term and long-term average ratio (STA/LTA CF) detector with the AIC function of higher order statistics. This algorithm could lock on the phase arrival time with a higher degree of accuracy by comparing the auto-picks with the analyst picks. Then we focused on the applicability of both the τ_c and CAV parameters for EEW and compared the performance of these parameters as magnitude estimators. Many records of the aftershocks provided us with basic data for making systematic investigation on the relationship between the parameters and magnitudes.

2. Seismic Data

The western area of China is the major earthquake zone where events happened of high seismic intensity and frequencies. The 2008 M_s 8.0 Wenchuan earthquake had generated 383 aftershocks by the end of 30 September 2008, which were facilitated by the China Strong Motion Net Centre (CSMNC) [7]. More than 600 events with magnitudes larger than M_s 4.0 were acquired, among them 56 aftershocks were above M_s 5.0 and 8 aftershocks, larger than M_s 6.0. These events were over a rupture length of about 300 km with focal depths ranging from 2 to 20 km.

We selected the main-shock and 37 aftershocks for this study. The selection criteria were $M_s > 4.0$ and for each earthquake at least three records were available within 150km of the hypocenter, which could ensure a good station coverage for each event and avoid path effects for P wave detection at longer distances. Thus we used 256 acceleration waveforms with good qualities, all the recorded were obtained by the strong motion seismographs with a dynamic range of $\pm 2g$ mainly installed at free-field sites and the sampling rate was 200 samples per second. The seismic events demonstrated a large range of focal depth and mechanisms vary from thrust to strike-slip that may affect the ray path, angle, and spectral content.

The direct current component was removed from the acceleration records by subtracting their mean value and the signals were integrated to velocity records, and then converted to displacement records. Following the analysis of Wu and Kanamori [4], we applied a 0.075 Hz Butterworth band-pass filter with four poles at the corner frequencies on the vertical component to remove the long-period drift after the numerical integration.

3. Automatic Picking Algorithm for P Waves

The detection of P waves was organized into two steps. In the first step the short-term and long-term average ratio (STA/LTA CF) detection algorithm described by Allen [8] was adopted. With two moving time windows, the event was detected when the ‘characteristic function’ of the short term is greater than that of the long term multiplied by some threshold values along the time. The CF is generally something that combines amplitude and frequency and the expression of the STA/LTA CF can be rewrite as follow

$$\frac{STA(i)}{LTA(i)} = \frac{\sum_{i+1-ns}^i CF(i)/ns}{\sum_{i+1-nl}^i CF(i)/nl} \quad (1)$$

where ns is the number of samples with the short-term moving window and nl is that of the long-term moving window. The STA/LTA CF detector can effectively reduce the erroneous picks.

The sampling rate may affect the length of the moving time windows; if the time window length is too large, it may lead to a smoother CF that little but important signal changes will be submerged; on the contrary, if the time window length is too short, it may cause erroneous picks due to the amplitude changings with every small interval. Through a trial-and-error process of the dataset, we set the time windows length as $STA=0.5$ sec, $LTA=5$ sec, and threshold value for P wave detections as $T_p=5$.

We used this STA/LTA CF function to detect P wave in the first step and regarded this initial picking time as T_1 . Because the high precise phase detection can improve the estimation of the expected magnitude and epicentral location of an event, we applied the AIC function combined with the kurtosis analysis in the second step.

According to Maeda [9], the onset estimation is corresponding to the global minimum of the AIC function in terms of a given seismic data $x(i)$ ($i=1,2,\dots,L$).

$$AIC(k) = k \cdot \log\{\text{var}(x[1,k])\} + (L-k-1) \cdot \log\{\text{var}(x[k+1,L])\} \quad (2)$$

where k ranges through all the seismogram samples in a certain window and $\text{var}(\ast)$ is the variance that defines the mean power of the alternating part of an ergodic process.

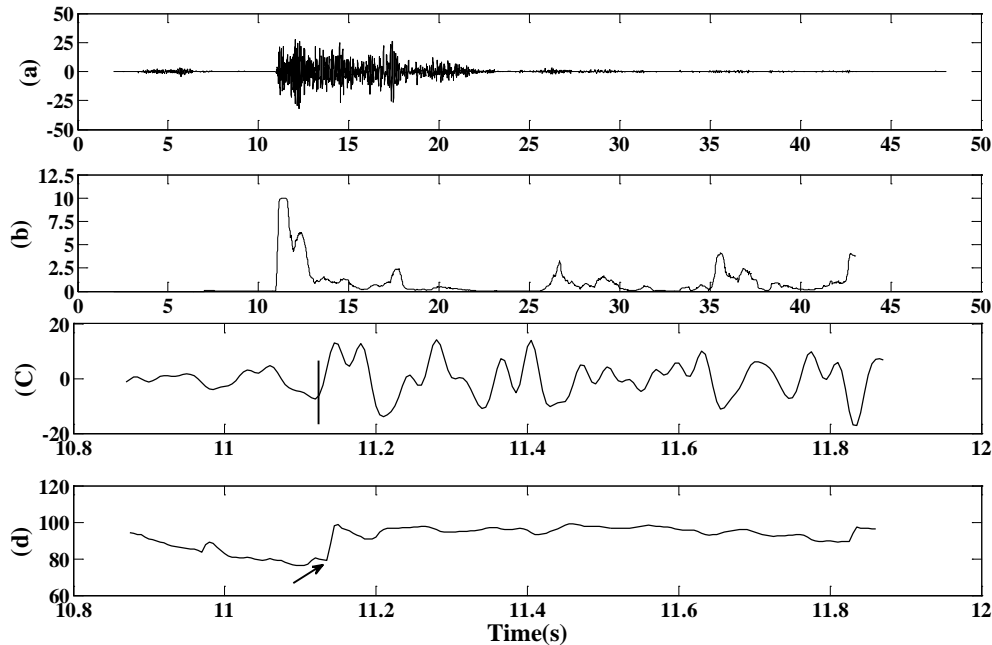


Fig. 1 – (a) Example of a seismogram; (b) the STA/LTA CF function; (c, d) the phase arrival is indicated by a vertical line corresponding to the AIC value of the global minimum indicated by an arrow.

Most of the noise is Gaussian distribution while the seismic-wave onsets temporarily generate a non-Gaussian distribution, thus the increased variance could lead to the detection of the onset times. However, compared with the variance analysis which is the lowest central moment quantifying the variability of a random variable, the higher order statistics demonstrate the essential superiority of detecting abrupt changes, especially the kurtosis function. Therefore in the second step, we substituted the kurtosis for variance in the AIC picker over a time window $[T_1-0.5, T_1+0.5]$ to refine the initial pick of each record. Fig. 1 shows an example of a seismogram and the STA/LTA pick (Fig. 1a, b) with its corresponding AIC value within the preliminary time window, there is a very clear global minimum that indicates the phase arrival (Fig. 1c, d).

We applied this detection method with the seismic data and evaluated the accuracy of the automatic picker by comparing the time differences between the analyst picks and the auto-picks for each record. Among the results, typical examples of the automatic and manual picks for an event is shown in Fig. 2.

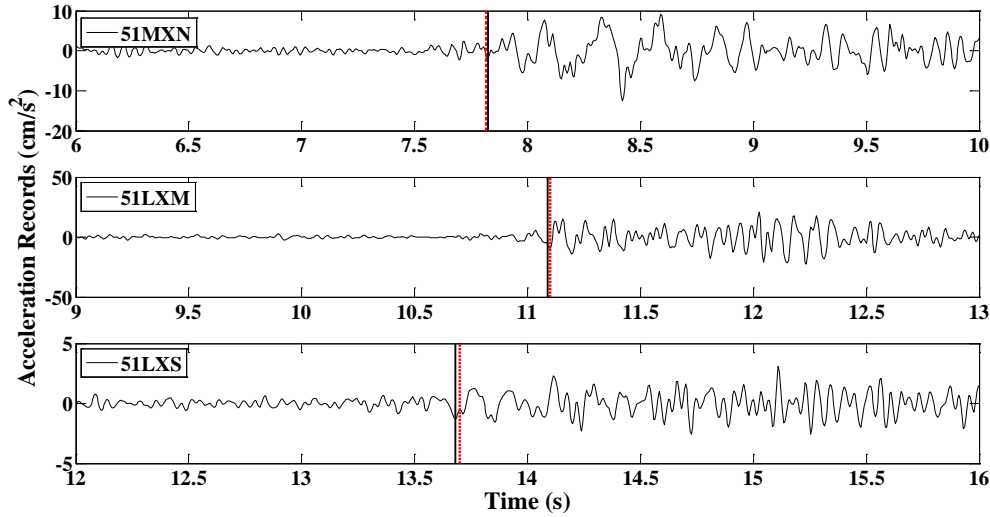


Fig. 2 – Example of the automatic picks and analyst pick for P waves, where three stations are illustrated. The dashed red line indicates the manual pick and the black solid line indicates the automatic pick.

Based on the records, about 95% of P wave arrivals were detected correctly, among which about 89% were within 0.1 sec of manual picks. The mean value and the standard deviation of the difference were -0.021 and 0.068 sec, respectively. Thus the combination method of the STA/LTA CF and the kurtosis-AIC function can significantly improve the detection of the P waves where the accuracy can fulfil the requirement of the EEW.

4. Magnitude Estimation

4.1 The τ_c Method

τ_c is a measure of the average period of ground motion over some specified time window and is obtained from the first several seconds after the arrival of P wave t_i :

$$\tau_c = 2\pi \sqrt{\int_{t_i}^{t_i+\tau_o} u^2 dt / \int_{t_i}^{t_i+\tau_o} v^2 dt} \quad (3)$$

where u is the high-pass filtered displacement of the vertical component ground motion and v is the velocity record. τ_o is the time duration of calculating the τ_c parameter and was set as 3 seconds herein. τ_c approximately represented the P wave pulse width and was found to correlate with the magnitude [3].

We averaged τ_c over the available waveform records of each event and established the linear relationship between M_s and the averaged τ_c by the least squares. Fig. 3 shows τ_c for all the events of the dataset by blue open circles, and the averaged τ_c values are in black solid circles. The regression relation is illustrated with red

solid line while the two black dashed lines indicate the range of one standard deviation, which shows a good correlation between the averaged τ_c and magnitude. The result was overall correlated with the one obtained for earthquakes in Japan, southern California, and Taiwan [4], except for the slight difference of the slope between τ_c and magnitude. Because the Wenchuan earthquake occurred in a region with a longer recurrence time compared with other areas.

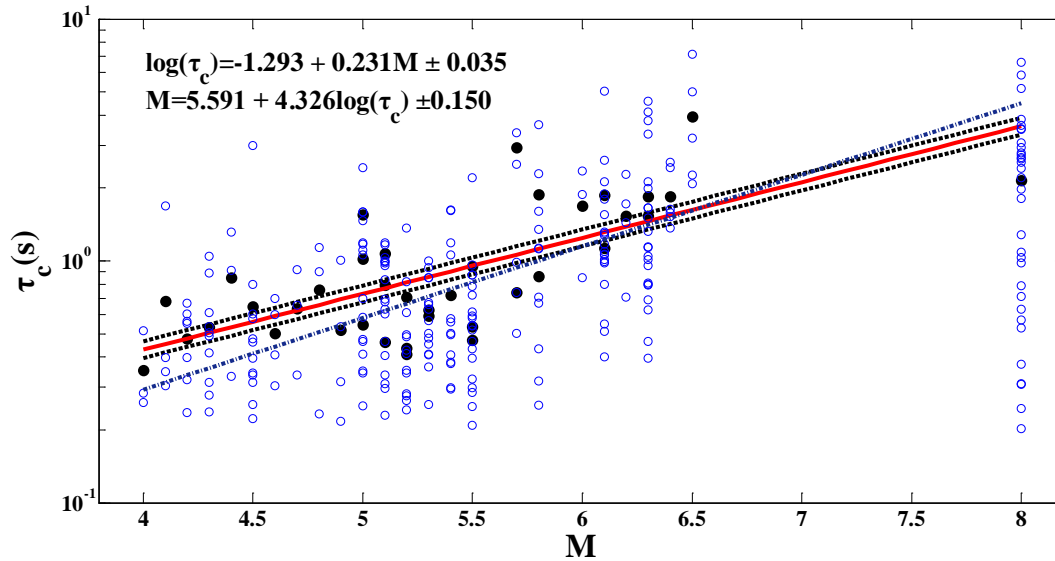


Fig. 3 – τ_c calculated from the first 3 second of P wave (blue open circles) and the averaged τ_c values (solid black circles). The τ_c vs. magnitude regression relation determined by our study is shown by red solid line with its standard deviations shown by black dashed lines. The result from Wu and Kanamori is shown by blue dashed-dotted line for comparison.

We also established the empirical relation using τ_c from single station where $\log(\tau_c) = -1.01 + 0.161 \times M \pm 0.09$, however it is obvious that the scatter is much larger than that of the averaged τ_c being used; meanwhile, the averaged τ_c has a larger slope vs. magnitude, which is good for magnitude estimation.

4.2 The CAV Method

CAV is a parameter for determining the damage threshold for engineering constructions subjected to earthquake ground motion. The CAV parameter is computed as the sum of the consecutive peak-to-valley distances in the velocity time history, and is defined as

$$CAV = \int_{t_i}^{t_i + \tau_o} |a(t)| dt \quad (4)$$

where, $a(t)$ is acceleration time history, and τ_o is the duration of record. In this study the time window used was 3 seconds for similarity with τ_c , the linear relation was shown by the least-squares fit between M_s and the averaged values of CAV from the available records for each earthquake.

Fig. 4 shows CAV values for the main-shock and 37 aftershocks in this study. While CAV increased with M_s within certain limits, as indicated by the corresponding standard deviation, which was lower than that of the average period, thereby indicating that the CAV might be influenced by the frequency content of ground motion.

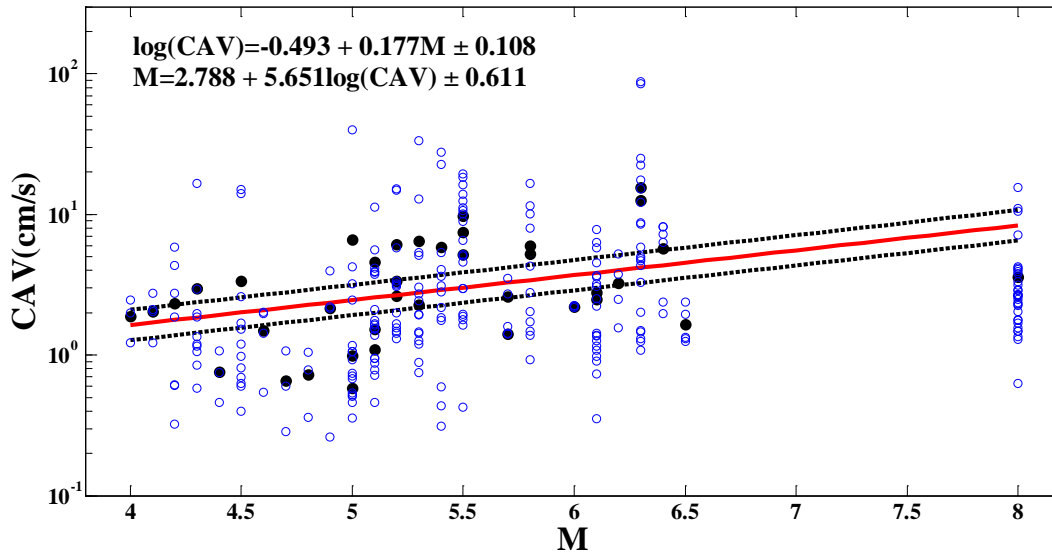


Fig. 4 – CAV calculated from the first 3 second of P wave (blue open circles) and the averaged CAV values (solid black circles). The CAV vs. magnitude regression relation determined by our study is shown by red solid line with its standard deviations shown by black dashed lines.

4.3 Application for Earthquake Early Warning

With the regression relationships between the two parameters and the magnitude available, we can estimate the magnitudes from the averaged τ_c and CAV by Eq. (5) and (6) obtained above:

$$M = 5.591 + 4.326 \times \log(\tau_c) \pm 0.150 \quad (5)$$

$$M = 2.788 + 5.651 \times \log(\text{CAV}) \pm 0.611 \quad (6)$$

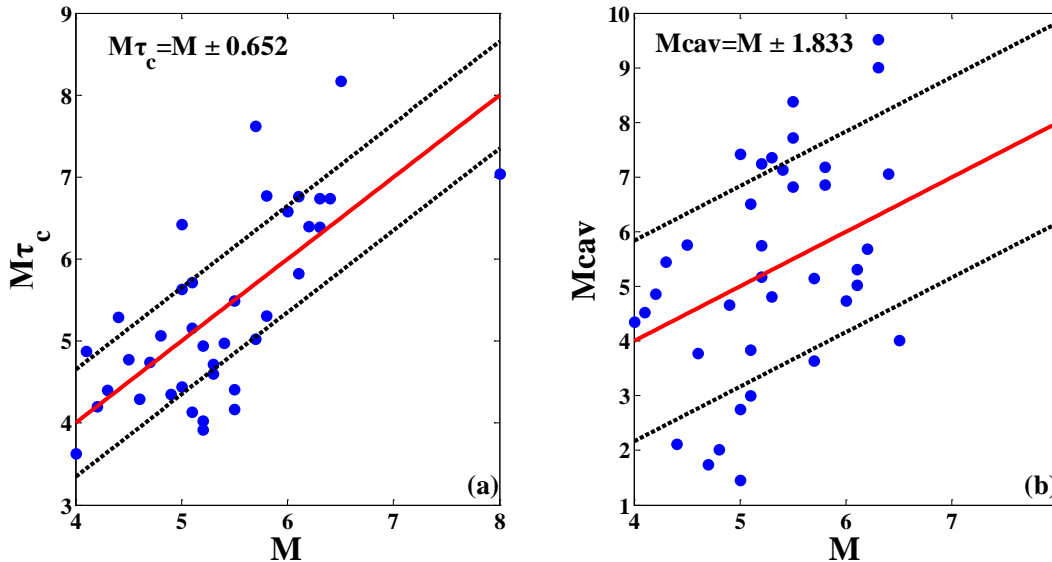


Fig. 5 – Magnitudes determined from τ_c (a) and CAV (b) versus the reported magnitude M. Solid line shows the least squares fit and the two dashed lines show the range of one standard deviation.

Fig. 5 compares the τ_c magnitudes and CAV magnitudes of the main-shock and 37 aftershocks with their catalogue magnitudes. On the 45° red line, $M_{\text{Parameter}}=M$, and the black dashed lines show the one standard deviation locations. Based on the results, τ_c seems more robust than CAV because of its smaller scatter.

For the aftershocks less than 6.5, the small uncertainty of magnitude estimation from both parameters suggested a consistency with the earthquake initiation model that the earliest stage of the rupture process could partially control the overall magnitude of an earthquake [5]. Thus the τ_c and CAV determined from the first 3 second P waves could provide reliable estimates for regional earthquake monitoring purpose and EEW operations.

However, the determinations of the main-shock from the parameters were both lower than its catalogue magnitude, with τ_c magnitude of 7.04 and CAV magnitude of 5.91, illustrating the saturation problem of magnitude estimations for large earthquakes, where the earthquake initiation model [5] may not be applicable to large earthquakes.

5. Discussion and Conclusion

The western area of China is of very complicated geological structure and topographic change, thus the 2008 M_s 8.0 earthquake happened on these faults had complex focal mechanism, propagation process and site effect, causing the ground motions to have the nature of complexity. The strong ground motion records were beneficial for us to develop the P wave detection algorithms and study the reliable magnitude determination parameters.

Since accurate picking of P arrival is essential for subsequent real-time analysis, we combined the preliminary detection of STA/LTA CF method with the kurtosis-AIC function, forming a double-process method. The automatic picks were compared with the analyst picks, showing that the accuracy could fulfill the requirement of the EEW.

We calculated τ_c and CAV for the selected main-shock and 37 aftershocks for this study and established the regression relationships between the two parameters and the magnitudes, respectively. Magnitudes were well correlated with the τ_c and CAV to a certain extent as indicated by the standard deviation, meaning that it was reliable to estimate the magnitude by using the ground motion parameters inferred from a robust database. In addition, the regression line of τ_c vs. magnitude of the Wenchuan earthquake was almost consistent with the equation proposed by Wu and Kanamori, suggesting that the average ground motion period could be a reliable and robust estimator for a wide range of regions.

However, the fitted line for magnitude with τ_c was better than that for magnitude with CAV, it might because CAV was obtained by numerical integration, the spread of the site conditions for stations may have affected it by modifying the acceleration amplitudes in each frequency band, thus the CAV was better at distinguishing whether the earthquake ground motion has potential damage or not. Both of the parameters illustrated saturation problem, suggesting that 3-second time window for them were not enough to estimate the earthquakes of large magnitude, where a longer time window was required.

As shown in this paper and many other papers, τ_c and CAV can provide a quick estimation of the magnitude and are among the most important parameters for early warning systems.

6. Acknowledgements

This research has been supported by the National Natural Science Foundation of China (No.U1434210, No.51278045 and No.40674016), the Science and Technology Promotion Project of China Ministry of Railway (No. 2010G018-C-1), the Project of Shenzhen Metro Group Co., Ltd (No. SZ-CGM-KY001/2014).

7. References

- [1] Allen RM, Gasparini P, Kamigaichi O, and et al (2009): The status of earthquake early warning around the world: An introductory overview. *Seismological Research Letters*, **80** (5), 682-693.

- [2] Wu YM, Kanamori H (2005): Experiment on an onsite early warning method for the Taiwan early warning system. *Bulletin of the Seismological Society of America*, **95**, 347-353.
- [3] Kanamori H (2005): Real-time seismology and earthquake damage mitigation. *Annual Review of Earth and Planetary Sciences*, **33**, 195-214.
- [4] Wu YM, Kanamori H (2008): Development of an earthquake early warning system using real-time strong motion signals. *Sensors*, **8** (1), 1-9.
- [5] Olson EL, Allen RM (2005): The deterministic nature of earthquake rupture. *Nature*, **438**, 212-215.
- [6] Erdik M, Fahjan Y, Ozel O, Alcik H, Mert A, Gul M (2003): Istanbul earthquake rapid response and the early warning system. *Bulletin of Earthquake Engineering*, **1**, 157-163.
- [7] China Strong Motion Networks Center (www.csmnc.net), [Accessed 05 November 2015].
- [8] Allen RV (1978): Automatic earthquake recognition and timing from single traces. *Bulletin of the Seismological Society of America*, **68**, 1521-1532.
- [9] Maeda N (1985): A method for reading and checking phase times in auto processing system of seismic wave data. *Zisin*, **38**, 365-379.